JOURNAL OF
ENVIRONMENTAL HYDROLOGY
The Electronic Journal of the International Association for Environmental Hydrology
On the World Wide Web at http://www.hydroweb.com
VOLUME 17 2009

SPATIAL DISTRIBUTION OF LATENT HEAT FLUX FROM LANDSAT (ETM+) SIMAGES

Juliano Schirmbeck[1]
Raúl Rivas[1,2]
Eduardo Usunoff[1,2]

[1]Instituto de Hidrología de Llanuras
Tandil, Buenos Aires, Argentina
[2]Comisión de Investigaciones Científicas
de la Provincia de Buenos Aires, Argentina

This paper describes the methodology used for estimating the latent heat flux (LE) by means of the energy balance equation and using data from Landsat EMT+ images. The aim of the application is to assess the LE distribution in an agricultural region located in the center of Buenos Aires Province, Argentina. The methodology made use of two images captured in November and December 2001, which correspond to the period of greatest demand in terms of evaporation and transpiration. The results from the image processing are quite consistent as compared to a local-scale Penman-Monteith model. Moreover, the maps obtained show variations of up to 3 mm/day among neighboring plots, a fact that is not detected by the local-scale model.

INTRODUCTION

The ever-increasing demand for water and the worldwide scarcity of water resources dictate the need for a correct modeling of hydrological systems to achieve a sustainable use of groundwater resources. These models are based on the balance between the water that enters and leaves the hydrogeological system. Evapotranspiration (ET) is a major process as far as the water that exits the system. Scientific advances for estimating the ET at a local scale have been very significant, although obtaining ET values at larger scales becomes difficult because of the large amount of information required.

Nowadays, remote sensing (RS) represents one of the most attractive tools for researchers and technicians who are interested in assessing the spatial and time-related evolution of various natural systems. Data from RS can be used for determining earth surface geophysical parameters, including albedo, emissivity, soil heat flux, surface temperature, and latent heat flux, that are very useful for estimating the regional scale energy balance (EB) (Boegh et al., 2002; Friedl, 2002; Sobrino et al., 2004; Kustas et al., 2004; Wang et al., 2006; Schirmbeck and Rivas, 2007b; Timmermans et al., 2007; Sánchez et al., 2007). Calculation of the latent heat flux is critical to determine the energy available for the ET process.

The objective of this paper is the assessment of the spatial distribution of ET from the EB that makes use of RS data and meteorological data. The RS information come from data captured by the Enhanced Thematic Mapper Plus (ETM+, mission Landsat 7) sensor.

METHODOLOGY

The EB consists of the distribution of the net radiation (*Rn*) at the surface, the soil heat flux (*G*), the sensible heat flux (*H*), and the latent heat flux (*LE*) (Timmermans et al., 2007):

$$Rn + G + H + LE = 0 \tag{1}$$

where the units of Equation 1 are energy per square meter.

The *Rn*, *G*, and *H* terms of Equation 1 are easily estimated from RS data (Boegh et al., 2002; Friedl, 2002; Kustas et al., 2004; Sobrino et al., 2005; Wang et al., 2006; Schirmbeck and Rivas, 2007b; Timmermans et al., 2007; Sánchez et al., 2007), whereas *LE* in most cases is estimated as the residual term.

In processing the Landsat images, the first step was to transform the digital values of the different bands into physical parameters for the top of the atmosphere (TOA). Bands 1 to 5 and 7 were converted into radiance and reflectance at the TOA, and band 6H (H meaning high radiometric resolution) into radiance and temperature following the findings of Schirmbeck and Rivas (2007a). The next step was the calculation of the EB terms, as will be shown below.

Net radiation (*Rn*) estimation

The *Rn* was calculated from the albedo (α), the emissivity (εs), and the surface temperature (*Ts*) with data of the ETM+ sensor, as well as local meteorological information. Local data used are the air temperature (*Ta*) and the incoming solar radiation ($Rs\downarrow$), which were measured at the same time that the image was captured (Friedl, 2002; Schirmbeck and Rivas, 2007a; Timmermans et al., 2007) (Equation 2):

$$Rn_i = Rs_{\downarrow}(1-\alpha) + \varepsilon s \varepsilon a \sigma Ta^4 - \varepsilon s \sigma Ts^4 \tag{2}$$

where *s* is the Stefan Boltzmann constant.

The air emissivity (ε_a in Equation 2) calculation used an expression that depends on *Ta* (Brutsaert, 1984):

$$\varepsilon_a = 0.92 \cdot 10^{-5} T_a^{\ 2} \tag{3}$$

Bands 1, 3, 4, 5, and 7 of the ETM+ sensor were used to calculate *a* (Liang et al., 2002):

$$\alpha = 0.356 \cdot \rho_{B1} + 0.130 \cdot \rho_{B3} + 0.373 \cdot \rho_{B4} + 0.085 \cdot \rho_{B5} + 0.072 \cdot \rho_{B7} \tag{4}$$

where ρ_{Bi} is the reflectivity of the *i*th band.

The emissivity at the surface for each pixel was estimated as follows (Sobrino et al., 2004):

$$\varepsilon_{Ls} = \varepsilon_V \cdot P_v + \varepsilon_S \cdot (1 - P_v) \tag{5}$$

In Equation 5, ε_{Ls} calculation assumes that, for the band 6H wavelength, the vegetation emissivity (P_v) is 0.99 and the soil emissivity (ε_s) is 0.973 (Sobrino et al., 2004).

The vegetation cover estimation used the normalized difference vegetation index (NDVI), assuming that those pixels where the NDVI value is between 0 and 0.3 represent bare soil (P_v=0), values in the range of 0.3-0.6 are a lineal combination of two components (soil and vegetation), whereas pixels with NDVI values of 0.6 to 1 are attributed to vegetation presence (P_v=1) (Schirmbeck and Rivas, 2007a).

In order to correct the temperatures of the TOA for atmospheric effects, the mono channel equation proposed by Coll et al. (1992) was used:

$$T_S = T_\lambda + \frac{1-\varepsilon_{Ls}}{\varepsilon_{Ls}} \cdot Li + \frac{K_\lambda \cdot W \cdot (T_\lambda - T_a)}{\varepsilon_{Ls} \cdot \cos(\theta) \cdot \left(1 - \frac{K_\lambda \times W}{\cos(\theta)}\right)} - 2 \cdot \frac{1-\varepsilon_{Ls}}{\varepsilon_{Ls}} \cdot K_\lambda \cdot W \cdot (T_a + L_i - T_\lambda) \tag{6}$$

where T_l is the black body temperature measured by the sensor, L_i is a fitting parameter that has temperature units (K), K_l is the total atmospheric absortion coefficient ($cm^2\ g^{-1}$), *W* is the water vapor content in the atmosphere ($g\ cm^{-2}$), and *q* is the sensor observation angle.

Soil heat flux (*G*) estimation

The *G* term can be estimated as a fraction of the *Rn* that is proportional to the vegetation cover. The *G* calculation used the Modified Soil Adjusted Vegetation Index (MSAVI), which takes into account the radiation emitted by the soil and the vegetation (Sobrino et al., 2005):

$$G = Rn \cdot A \cdot \exp(-2.13 MSAVI) \tag{7}$$

The *A* constant determines the maximum fraction of *G* that is registered in a bare soil. For a typical soil of the Tandil area (Buenos Aires Province, Argentina), the*A* parameter takes on a value of 0.1 ±0.02 (calculated from an EB Campbell Scientific station for a 300-day period installed on a short grass plot). The MSAVI estimation used the following equation (Qi et al., 1994):

$$MSAVI = \frac{2\rho_{B4} + 1 - \sqrt{(2\rho_{B4} + 1)^2 - 8(\rho_{B4} - \rho_{B3})}}{2} \tag{8}$$

Sensible heat flux (*H*) estimation

The sensible heat flux (*H*) may be obtained from specific models that are based on one-dimensional energy flow, such as (Boegh et al., 2002; Kustas et al., 2004; Wang et al., 2006):

$$H = \rho c_p \frac{Ts - Ta}{ra} \tag{9}$$

where ρ is the air density, c_p is the specific heat of humid air at a constant pressure, and *ra* is the aerodynamic resistance.

Latent heat flux (*LE*) estimation

The daily *LE* has been estimated as a residual term of Equation 1. The change from instantaneous to daily values for net radiation may be obtained from the ratio between both values (*Rnd*/*Rni*). In this work, and according to Seguin and Itier (1983), *Rnd*/*Rni* = 0.3 ± 0.03. Therefore, *Rnd* can be written as:

$$Rnd = Rni \cdot 0.3 \tag{10}$$

Reference evapotranspiration (ET_o) estimation

As a way of checking the consistency of the *LE* estimates obtained from Equation 1, the reference evapotranspiration (ET_o) values were calculated. The daily ET_o took into account the records of three meteorological stations within the study area and the Penman-Monteith model (Allen et al., 1988):

$$ET_o = \frac{0.408 \cdot (R_N - G) + \gamma \cdot \frac{900}{273.16 + T_a} \cdot U_2 \cdot (e_a - e_d)}{\Delta + \gamma \cdot (1 + 0.34 \cdot U_2)} \tag{11}$$

where ET_o (mm d^{-1}), R_n (MJ m^{-2} d^{-1}), and G (MJ m^{-2} d^{-1}) have been defined, U_2 is the wind velocity (m s^{-1}), $(e_a - e_d)$ is the vapor pressure deficit (kPa), D is the slope of the vapor pressure curve (kPa °C^{-1}), γ is a psychrometric constant (kPa °C^{-1}), 900 is the coefficient for the reference crop (kJ kg K d^{-1}), and 0.34 is a dimensionless coefficient that comes from the ratio between the aerodynamic resistance and that of the reference crop.

RESULTS

The proposed methodology has been applied to two images (path-row 225-86) captured by the ETM+ sensor on November 21 and December 23, 2001. It may be important to mention that in 2001 the rainfall was 54% above the historical annual mean of 918 mm y^{-1}. Excess water was registered in November, and the local soils held a maximum water content (*ETmax*≅*LE*), whereas in December the rainfall was not abundant and the soils were below their maximum availability of water *ETmax*>*LE*).

The study area (Figure 1) is at the center of Buenos Aires Province, Argentina. It is within the so-called Humid Pampas, where agricultural activities (mainly cereal crops and oilseeds) are of primary importance. It is a rather flat plain with a mean annual rainfall of 918 mm y^{-1} and water excess during fall and spring seasons. The mean annual temperature is 15 °C, and the winter and summer seasons are quite different in terms of mean temperature. The wind has a mean velocity

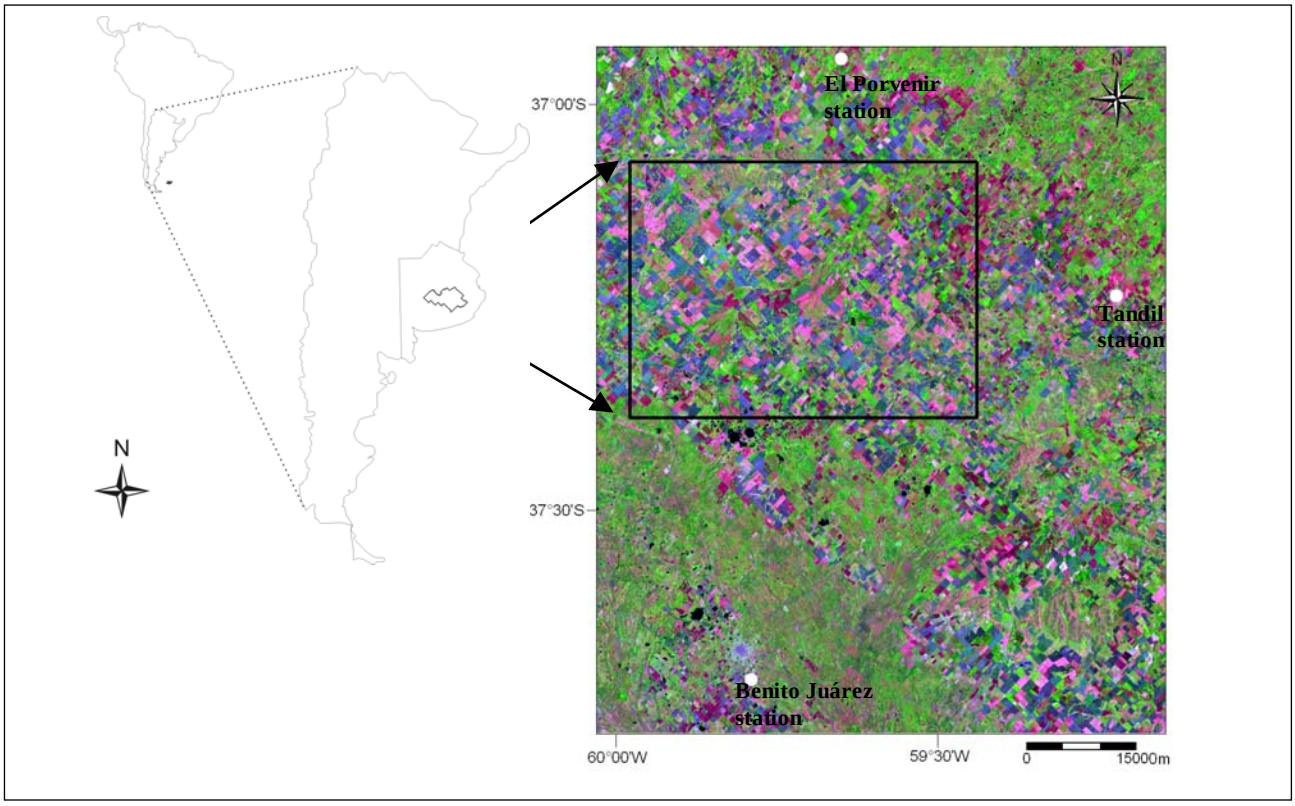

Figure 1. Location of the study area and the meteorological stations shown on a portion of band 4 (image 225-86 of December 23, 2001).

of 9 Km h^{-1}, and the average air humidity is 72%. According to Thornthwaite, the climate is classified as sub-humid/humid, mesothermal, with a low or null water deficit. Most of the water leaves the hydrological system as evapotranspiration (80-85% of the rainfall).

Figure 1 shows the study area and the location of the meteorological stations used for the *ETo* estimation. The stations are: El Porvenir (36.7 S, 59.1 W, 132 m), where hourly data are registered by an automatic Campbell Scientific ET106 station belonging to the Instituto de Hidrología de Llanuras (data of this station corresponding to the day/time of images captured were used for the EB models), and two stations operated by the National Weather Service, the Tandil station (37.2 S, 59.2 W, 175 m), and the Benito Juárez station (37.7 S, 59.7 W, 214 m).

Figures 2 and 3 present the ET maps obtained from the processing of the images captured on November 21 and December 23, 2001. The spatial variability of the evapotranspiration is between 2 and 8 mm day^{-1} (1 mm day^{-1} step). It can be seen that adjacent plots have differences of up to 3 mm day^{-1}.

One of the main advantages in estimating the *LE* from EB is that the values obtained correspond to the real energy used in the process of transferring the latent heat flux. For the November 21 image, when the soils hold the maximum amount of water available, the *LE* values are similar to the *ETo Kc* estimates, with differences less than 0.6 mm d^{-1} (Table 1, rows 1 and 2). For the December 23 image, when the water content of soils is below the vegetation requirements, the *LE* values are significantly smaller than those of the *ETo Kc*, showing the model ability to identify water stress situations (Table 1, rows 3 and 4).

These results show the ability of the method and its consistency for estimating the real loss of water (with and without water stress) from the plots considered in this study.

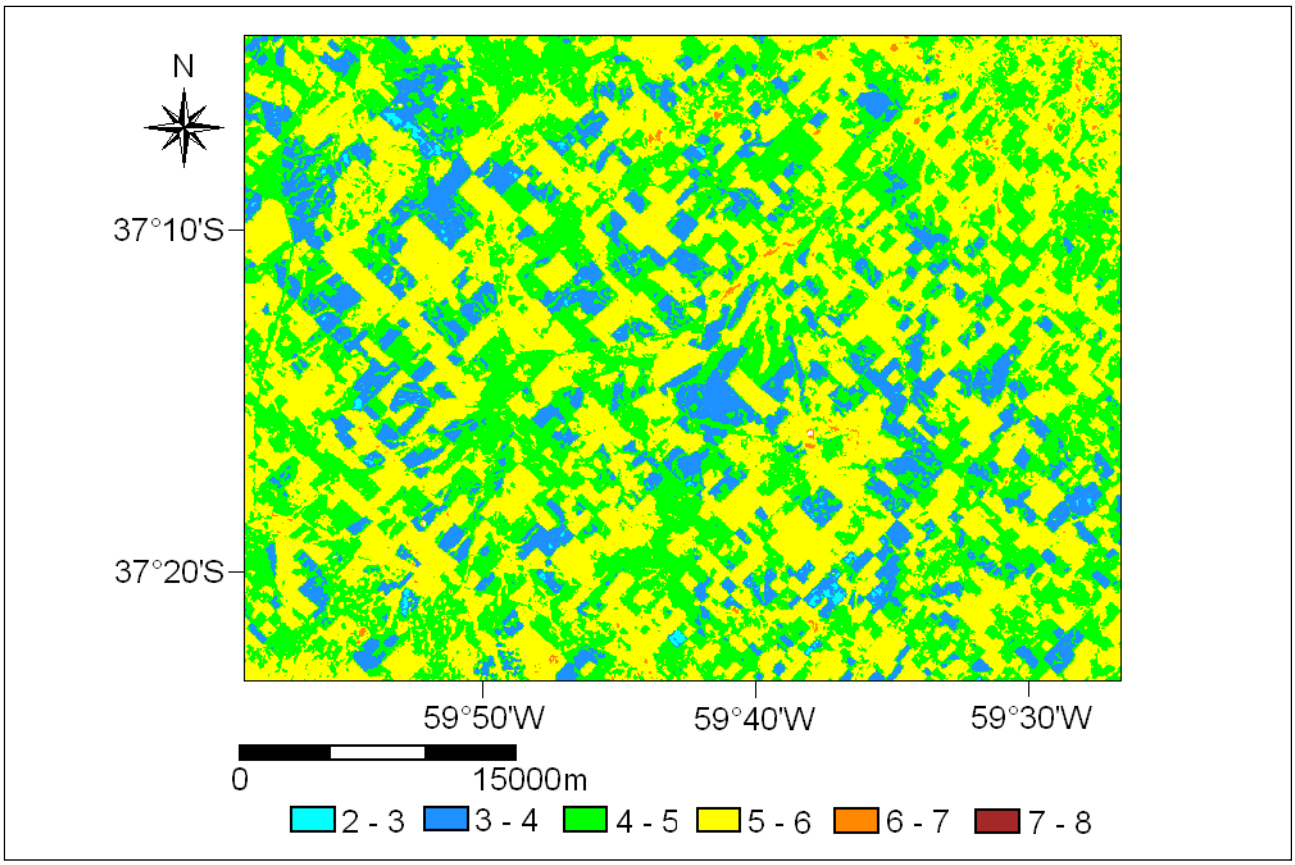

Figure 2. Latent heat flux (ET, mm d^{-1}) in the study area from the November 21, 2001 image.

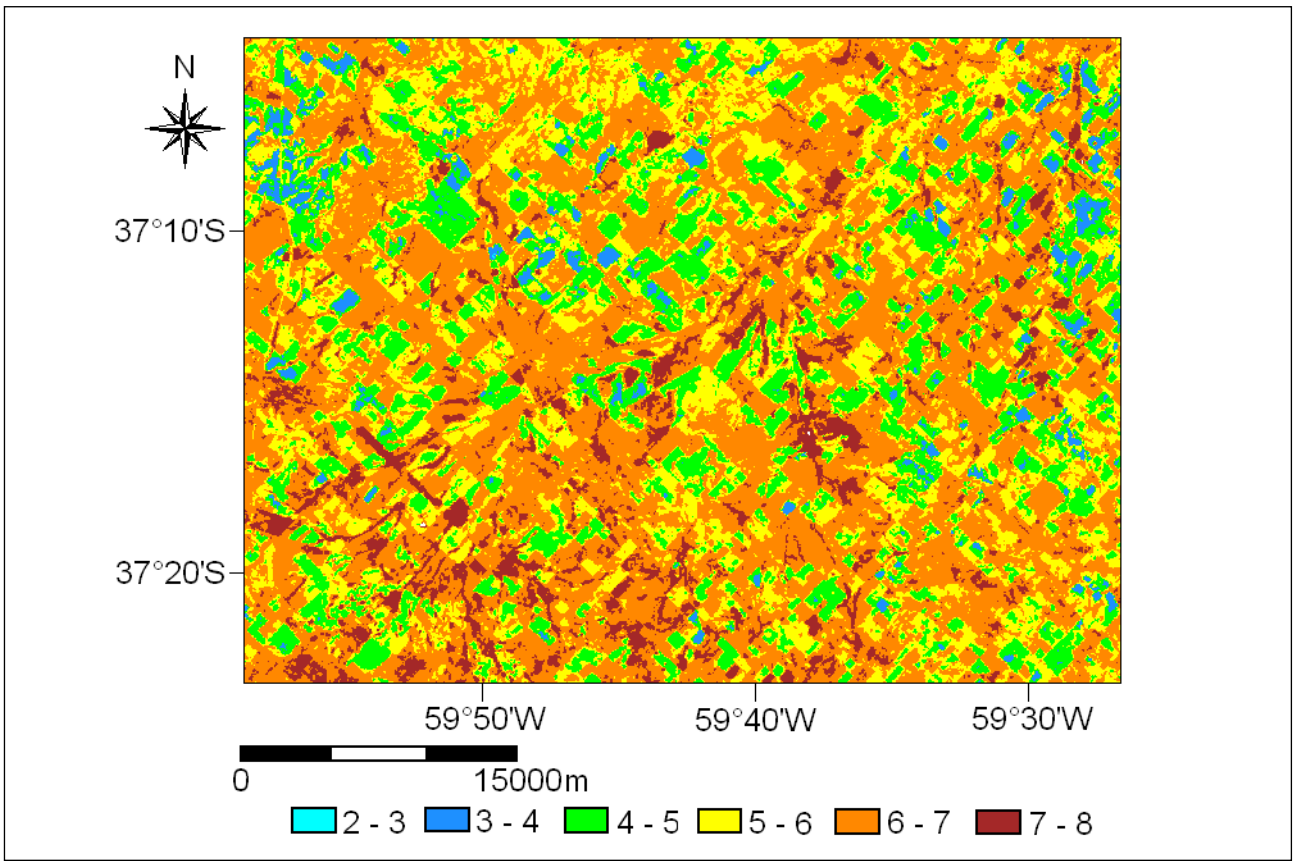

Figure 3. Latent heat flux (ET, mm d^{-1}) in the study area from the December 23, 2001 image.

Table 1. LE (mm d^{-1}) and ETo.Kc (mm d^{-1}) obtained from the meteorological stations data and from plots with vegetation cover near the stations from the image.

Station	Date	LE	ETo Kc
Benito Juárez	11/21/2001	5.0	5.6
Tandil	11/21/2001	5.2	5.6
Tandil	12/23/2001	6.1	7.1
El Porvenir	12/23/2001	6.3	8.5

CONCLUSIONS

This paper presents a simple method for the estimation of *LE* (evapotranspiration) from images captured by the ETM+ sensor. The *LE* maps are consistent with measurements taken at reference plots. Further, the detected spatial variability of *LE* for two different dates of high-water demand show an important variation of water loss from the soil-water-plant system.

The models used for estimating the components of the EB have been tested and the results obtained in the center of Buenos Aires Province, Argentina (Table 1) indicate that they can be usefully applied throughout the region.

The methodology can be very useful for hydrological studies at regional and field plot scales, including aquifer recharge assessment, estimation of crop water requirements, the quantification of net primary productivity, and the overall management of water resources.

ACKNOWLEDGMENTS

The authors would like to thank the Comisión de Investigaciones Científicas de Buenos Aires, Argentina and the Agencia Nacional de Promoción Científica y Tecnológica (Argentina) for the funds received to carry on their research projects.

The authors would also like to thank the comments and suggestions of their peers, which have greatly improved the quality of the methodological issues presented.

REFERENCES

Allen, R.G., L.S. Pereira, D. Raes, and M. Smith. 1998. Crop evapotranspiration-Guidelines for computing crop water requirements-FAO. Irrigation and drainage paper 56. Water Resources, Development and Management Service, Rome, Italy.

Boegh, E., H. Soegaard, and A. Thomsen. 2002. Evaluating evapotranspiration rates and surface conditions using Landsat TM to estimate atmospheric resistance and surface resistance., Remote Sensing of Environment, 79: 329 – 343.

Brutsaert, W. 1984. Evaporation into the atmosphere. Theory, history, and applications. Reidel Publishing Company, Dordrecht, Holland, 299 pp.

Coll, C., V. Caselles, and J.A. Sobrino. 1992. Desarrollo de un modelo de corrección atmosférica en el térmico. I Aplicación al canal 6 de Landsat. Anales de Física, 88: 107 – 119.

Friedl, M.A. 2002. Forward and inverse modeling of land surface energy balance using surface temperature measurements Remote Sensing of Environment, 79: 344 – 354.

Kustas, W.P., F. Li, T.J. Jackson, J.H. Prueger, J.L. MacPherson, and M. Wolde. 2004. Effects of remote sensing pixel resolution on modelled energy flux variability of croplands in Iowa. Remote Sensing of Environment, 92: 535 – 547.

Liang, S., H. Fang, M. Chen, C.J. Shuey, C. Walthall, C. Daughtry, J. Morisette, C. Schaaf, and A. Strahler. 2002. Validating MODIS land surface reflectance and albedo products: methods and preliminary results. Remote

Sensing of Environment, 83: 149 – 162.

Qi, J., A. Chehbouni, A.R. Huete, Y.H. Kerr, and S. Sorooshian. 1994. A modified soil adjusted vegetation index (MSAVI). Remote Sensing Environment, 48: 119 – 126.

Sánchez, J.M., W.P. Kustas, V. Caselles, and M.C. Anderson. 2007. Modelling surface energy fluxes over maize using a two-source patch model and radiometric soil and canopy temperature observations. Remote Sensing of Environment, 112: 1130 – 1143.

Schirmbeck, J., and R. Rivas. 2007a. Estimación de la radiación neta a nivel del suelo a partir de datos captados por el sensor ETM+. Anais del XV Simpósio Brasileiro de Sensoriamento Remoto: 6159 – 6165.

Schirmbeck, J., and R. Rivas. 2007b. Comportamiento de los términos del balance de energía en una pastura. Acta del XII Congreso de la Asociación Española de Teledetección.

Seguin, B., and B. Itier. 1983. Using midday surface temperature to estimate daily evaporation from satellite thermal IR data. International Journal of Remote Sensig, 4: 371 – 383.

Sobrino, J., J.C. Jimenez Muñoz, and L. Paolini. 2004. Land surface temperature retrieval from LANDSAT TM 5. Remote Sensing of Environment, 90: 434 – 440.

Sobrino, J., M. Gómez, J.C. Jiménez Muñoz, A. Olioso, and G. Chehbouni. 2005. A simple algorithm to estimate evapotranspiration from DAIS data: Application to the DAISEX campaigns. Journal of Hydrology, 315: 117 – 125.

Timmermans, W.J., W.P. Kustas, M.C. Anderson, and A.N. French. 2007. An intercomparison of the Surface Energy Balance Algorithm for Land (SEBAL) and the Two-Source Energy Balance (TSEB) modeling schemes. Remote Sensing of Environment, 108: 369 – 384.

Wang K., Z. Li, and M. Cribb. 2006. Estimation of evaporative fraction from a combination of day and night land surface temperatures and NDVI: A new method to determine the Priestley–Taylor parameter. Remote Sensing of Environment, 102: 293 – 305.

ADDRESS FOR CORRESPONDENCE
Juliano Schirmbeck
Instituto de Hidrología de Llanuras
Pinto 399
B7000GHG, Tandil
Buenos Aires, Argentina

Email: jschirmbeck@rec.unicen.edu.ar